



Draft Manuscript for Review

## Depths in a day - A new era of rapid-response Raman-based barometry using fluid inclusions

Journal:	<i>Journal of Petrology</i>
Manuscript ID	JPET-Nov-23-0174
Manuscript Type:	Letter
Date Submitted by the Author:	16-Nov-2023
Complete List of Authors:	Devitre, Charlotte; University of California Berkeley, Earth and Planetary Sciences Wieser, Penny; UC Berkeley, Earth and Planetary Science Bearden, Alexander; University of California Berkeley, Earth and Planetary Sciences Richie, Araela; University of California Berkeley, Earth and Planetary Sciences Rangel, Berenise; University of California Berkeley, Earth and Planetary Sciences Gleeson, Matthew; University of California Berkeley, Earth and Planetary Sciences Grimsich, John; University of California Berkeley, Earth and Planetary Sciences Lynn, kendra; US Geological Survey, Hawaiian Volcano Observatory Downs, Drew; US Geological Survey, Hawaiian Volcano Observatory Deligne, Natalia; US Geological Survey, Hawaiian Volcano Observatory Mulliken, Katherine; US Geological Survey, Hawaiian Volcano Observatory
Keyword:	fluid inclusions, geobarometry, raman spectroscopy, rapid response, volcano monitoring
Journal of Petrology now offers Virtual Collections of published papers. You may choose up to three collections from the list below. Virtual collections will increase the visibility of your work.:	Oceanic Intraplate Magmatism < Province Themes, Melt and Fluid Inclusions < Material Themes

SCHOLARONE™  
Manuscripts

1    **Depths in a day - A new era of rapid-response Raman-based**  
2    **barometry using fluid inclusions.**

3    Running title: Depths in a day – a new era of rapid response barometry


4


5    Charlotte L. DeVitre<sup>1\*</sup>, Penny E. Wieser<sup>1</sup>, Alexander T. Bearden<sup>1</sup>, Araela Richie<sup>1</sup>, Berenise  
6    Rangel<sup>1</sup>, Matthew LM Gleeson<sup>1</sup>, John Grimsich<sup>1</sup>, Kendra J. Lynn<sup>2</sup>, Drew T. Downs<sup>2</sup>,  
7    Natalia I. Deligne<sup>2</sup>, and Katherine M. Mulliken<sup>2</sup>


8    <sup>1</sup> Earth and Planetary Sciences, University of California, Berkeley, CA 94270, USA


9    <sup>2</sup> U. S. Geological Survey, Hawaiian Volcano Observatory, Hilo, HI 96720, USA

10    \* Corresponding author: Charlotte L. DeVitre [cl.devitre@gmail.com](mailto:cl.devitre@gmail.com)

11     ORCID (CLD): [0000-0002-7167-7997](https://orcid.org/0000-0002-7167-7997)

12     ORCID (KJL): 0000-0001-7886-4376

13     ORCID (DTD): 0000-0002-9056-1404

14     ORCID (NID): 0000-0001-9221-8581

15    Word count: Abstract 70, Main1705

## Abstract

Rapid-response petrological monitoring is a major advance for volcano observatories to build and validate models of the plumbing systems that supply eruptions in near-real-time. Our rapid-response analysis of tephra from the September 2023 eruption of Kīlauea shows that Raman analyses of fluid inclusions can robustly determine magma reservoir depths within a day of receiving samples – a transformative timescale for decision making that has not previously been achieved by petrological methods.

**Keywords:** Fluid Inclusions; Geobarometry; Raman Spectroscopy; Rapid Response; Volcano Monitoring

\* The use of trade names does not signify endorsement by the U.S. Geological Survey.

## Main Text

Volcano observatories increasingly use data collected from erupted lava and tephra samples in near-real-time to obtain information about the magmatic plumbing system to help inform decision making during volcanic crises (Gansecki *et al.*, 2019; Re *et al.*, 2021; Pankhurst *et al.*, 2022). Most work so far has focused on the chemistry of erupted lavas and crystal cargoes (Pankhurst *et al.*, 2022) to gain insight into changing melt composition and rheological properties (e.g., Gansecki *et al.*, 2019). However, up until now, petrological monitoring has been unable to address the high-priority question– ‘*Where is the magma coming from?*’ (Re *et al.*, 2021). At well-monitored volcanoes, such information can be used to draw analogies to previous eruptive episodes associated with specific storage reservoirs (e.g., vigour, pathway, or length of eruption), and to help interpret geophysical signals of ongoing activity. At poorly-monitored volcanoes, where there may be no prior constraints on magma storage geometry (Wieser *et al.*, 2023b), depths of storage are a vital parameter to begin interpreting new eruptive activity. Melt inclusion (MI) barometry, a widely popular petrological method to determine storage depths from volatile contents, takes months to years to complete (Re *et al.*, 2021). While mineral barometry could be implemented faster (only requiring electron probe microanalysis (EPMA) measurements on eruptive minerals), it is imprecise (Wieser *et al.*, 2023a), and therefore would only be able to constrain magma storage to very broad depths (e.g., stored in the crust vs. below the Moho). This technique has particularly poor applicability at active volcanoes such as Kīlauea or Mauna Loa, where a precision of 1–2

\* The use of trade names does not signify endorsement by the U.S. Geological Survey.

49 km is needed to distinguish between storage reservoirs (Baker and Amelung, 2012;  
50 Anderson and Poland, 2016).

51 Recent developments have shown that Raman-based barometry of CO<sub>2</sub>-rich fluid  
52 inclusions (FI) provides an alternative to popular petrological barometers, with much  
53 smaller uncertainties than mineral barometry, and requiring far less time and resources than  
54 MI analyses (Dayton *et al.*, 2023; DeVitre and Wieser, 2023). This method uses spectral  
55 features of CO<sub>2</sub> fluids to calculate a CO<sub>2</sub> density using an instrument specific calibration  
56 (DeVitre *et al.*, 2021). Along with an estimate of entrapment temperature, this density is  
57 converted into an entrapment pressure using a CO<sub>2</sub> Equation of State (EOS). Pressures are  
58 converted to depths through an estimate of crustal density. However, there has previously  
59 been no rigorous assessment of how quickly FI depths can be obtained from erupted  
60 material, and whether these timescales are short enough to have use as a real-time  
61 monitoring tool.

62 The eruption onset of Kīlauea volcano on September 10, 2023 provided an  
63 unprecedented opportunity to test the validity of this method during a response, given that  
64 depths of the main magma storage regions at this volcano have been well constrained by  
65 various independent geophysical and petrological methods, including prior FI barometry  
66 (DeVitre and Wieser, 2023). Tephra samples representing the first ~14 hours of the  
67 September 2023 eruption were collected by Hawaiian Volcano Observatory (HVO)  
68 geologists on September 12 and mailed to UC Berkeley on September 15<sup>th</sup> (Fig. 1).

69 Our simulation started on September 20 at 9 am PST (Day 1), the morning after  
70 sample receipt (Fig. 1). We used a production-line style workflow involving two  
71 undergraduates, a 1<sup>st</sup> year graduate student, a post-doc, and an assistant professor, with

\* The use of trade names does not signify endorsement by the U.S. Geological Survey.

stations for crushing and sieving, mineral picking, FI preparation, sample cataloguing, and analysis. The first steps were to crush and sieve tephra, pick olivine crystals (size fractions 0.5-1 and 1-2 mm) crystals, and begin mounting crystals in CrystalBond™\* to search for FI. By 2 pm PST (5 hrs into the simulation), we had collected our first Raman spectra. By ~7 pm PST, we had processed the spectra from 16 FI to get CO<sub>2</sub> densities using a calibration relating CO<sub>2</sub> density to Fermi level separation (DeVitre and Wieser (2023), DeVitre et al. 2021). CO<sub>2</sub> densities were converted into pressures using the EOS of Pan and Wagner, 1996), assuming an entrapment temperature of 1150 °C. Pressures were converted into depths using the crustal density model of Ryan, (1987) parameterized by Lerner *et al.* (2021). We shared the resulting histogram (Fig 2a) of storage depths with HVO collaborators showing that crystals, and thus magma, were likely coming from the shallower Halema'uma'u reservoir of Kīlauea (HMM on Fig. 2a–b). It worthwhile to note that the number of FI reported on Day 2 is comparable to many melt inclusion studies, which often aim for ~20 MI per sample but frequently report fewer (e.g., Lerner *et al.*, 2021) reported 14 MI with sufficient data – that is MI glass total volatile contents and major element compositions - to produce saturation pressures for the LERZ eruption of 2018). We also had an additional ~20 FI fully prepared and catalogued for analysis by the end of Day 1.

On Day 2, these 20 FI were analysed, while supplementary FI were prepared and catalogued. After analysis of ~15 crystals hosting FI, these crystals were passed from the Raman to a workstation where they were removed from CrystalBond™ and placed on tape to make an epoxy mount. Epoxy was poured at the end of the day. By ~8:30 pm PST on Day 2, we shared an updated histogram of 46 FI pressures and depths, confirming the

\* The use of trade names does not signify endorsement by the U.S. Geological Survey.

dominant contribution of the Halema‘uma‘u reservoir (Fig. 2a and c). On Day 3, while waiting for the epoxy to fully set, we finished analysing prepared FI. Then we polished the mount and began cataloguing the regions of crystals on which to perform energy-dispersive spectroscopy (EDS). On Day 4, olivine forsterite contents ( $Fo = 100 \cdot Mg / (Mg + Fe)$  molar) were determined by EDS, providing a framework to further interpret the plumbing system (Fig. 2d). The Fo content of an olivine is a function of MgO and FeO in the liquid and the Ol-Liq partitioning coefficient ( $K_D$ ). Thus, the Fo contents of the host olivine close to each FI can be used to assess the calculated storage depth in its broader petrographic context (e.g., distinguishing high-Fo olivines which crystallize from more primitive melts from low Fo olivines forming in more evolved melts). This olivine forsterite content can also be used to estimate the likely entrapment temperature of each fluid inclusion (see DeVitre and Wieser, 2023) for performing EOS calculations, rather than having to use a uniform temperature as on Day 1-2.

Our results clearly show that the majority of FI were entrapped at ~1–2 km below the surface (Fig. 2d), which aligns well with the depths of the Halema‘uma‘u reservoir interpreted from geophysics (Baker and Amelung, 2012; Anderson and Poland, 2016; Anderson *et al.*, 2019), MI barometry (Lerner *et al.*, 2021; Wieser *et al.*, 2021), and FI barometry (DeVitre and Wieser, 2023). While the greater number of analyses from data processed on Day 2 and Day 4 certainly enhance the story, it is notable that depths calculated on Day 1 fall within final proposed storage reservoir depths. Rapid EDS analyses of olivine Fo contents close to each FI reveal that olivine crystals grew from a wide range of melt compositions. It is interesting to note that FI in the cores of high-Fo (e.g., >86) olivine crystals return pressures indicative of the shallower Halema‘uma‘u

\* The use of trade names does not signify endorsement by the U.S. Geological Survey.

reservoir since it has been suggested in previous eruptions that these high-Fo olivine crystals predominantly grow in the deeper South Caldera reservoir (SC on Fig. 2a), where high MgO melts are thought to reside (Helz *et al.*, 2014; Pietruszka *et al.*, 2015, 2018; Wieser *et al.*, 2019). We suggest three possible scenarios to explain the relatively shallow pressures documented in high-Fo olivine crystals:

1) FI in high-Fo olivine crystals were entrapped within the South Caldera reservoir and then transported into the Halema'uma'u reservoir, where the fluid inclusions re-equilibrated to lower pressures prior to eruption over shorter timescales than would be required to reset the host Fo content.

2) High-MgO melts were injected into the Halema'uma'u reservoir, where high-Fo olivine crystallized and trapped FI at shallow depths.

3) Complex skeletal growth of olivine crystals during extensive undercooling (e.g., (Welsch *et al.*, 2013) could mean that high-Fo olivine cores, which initially grew in the SC reservoir texturally evolved and trapped lower pressure FI in the Halema'uma'u reservoir.

We think that scenario 1 is unlikely given the that FI from the 2018 lower East Rift Zone eruption appear not to have re-equilibrated despite stalling in the Halema'uma'u reservoir for up to 2 years (DeVitre and Wieser, 2023; Mourey *et al.*, 2023), and our models of FI re-equilibration indicate <10% change in pressure over this time period. Current data does not allow us to resolve scenario 2 vs 3, but this eruption could provide an opportunity to explore this further (e.g., through detailed Phosphorous mapping in olivine around FI). Regardless of the exact mechanism, our FI pressures indicate that erupted crystal cargo experienced storage at Halema'uma'u reservoir depths prior to eruption, and thus this was the most probable reservoir supplying magma to the surface in the Sept 2023 eruption.

\* The use of trade names does not signify endorsement by the U.S. Geological Survey.



This simulation shows that Raman-based FI barometry has significant potential for rapid-response petrological monitoring globally. It could be applied to any CO<sub>2</sub>-rich volcanic system – which includes numerous hazardous and frequently active volcanic regions worldwide (e.g., Galápagos, Réunion, Azores, Canary Islands, Iceland, Cabo Verde). The resources and personnel required are modest. Sample preparation was carried out using transmitted-reflected light microscopes from the University of California teaching collection, only using a research-grade microscope for sample cataloguing. Raman spectrometers are widely available at many universities, given that it is a popular technique in many other fields, such as material sciences, physics, chemistry, and biology, and the W-filament SEM used for EDS analyses to get olivine Fo contents has been around for 15 years (See Supplementary Information S1 Appendix).

This simulation also enabled us to identify several ‘bottlenecks’ in this rapid-response workflow (yellow stars, Fig. 1, see Supplementary Information S1 Appendix for further details) so that we could determine depths even faster during future eruptions:

- 1) No courier services ship packages out of Hilo, Hawai‘i over the weekend, and estimated delivery days are not reliable.
- 2) The epoxy took 18 hours to cure enough for polishing (vs. 8 hours on the datasheet). Faster curing epoxies can be used to eliminate this delay.
- 3) We spent significant time cataloguing samples on a research-grade microscope to help navigate on the Raman microscope, but later realized that smartphone cameras with teaching microscopes would have worked faster.

Overall, we have demonstrated that a modest-sized research group with prior teaching and class commitments working without overnight shifts can obtain pressures on relevant

\* The use of trade names does not signify endorsement by the U.S. Geological Survey.

timelines for understanding volcanic plumbing systems during periods of unrest. This technique adds valuable quantitative storage depth information that expands on HVO's routine near-real-time chemical monitoring with bulk rock ED-XRF (Gansecki *et al.*, 2019). In a true eruptive crisis, magma storage depths could be obtained even faster by removing bottlenecks 1–3, implementing overnight shift work, and requesting teaching release and class absences for students.

### Author contributions

Author contributions for lab work are shown on Fig. 1. CD and PW wrote the paper. CD, PW, AR, BR, and AB prepared tephra, picked olivine, found FIs, catalogued them, mounted them, and conducted Raman analyses. CD and PW performed all spectral fitting, data processing, and figure making, with schematic illustrations shown in Fig. 1 from AB. JG developed the Mg/Fe calibration for the EDS detector and MG performed EDS analyses with help from JG. KJL, DTD, NID and KMM collected samples, processed them in Hilo, and provided eruption context. KJL and DD prepared the glass mount and did the EMPA analyses.

### Acknowledgements

PW and CD acknowledge support from NSF EAR 2217371 and the Berkeley Rose Hills Innovator Program. Any use of trade, product, or firm names is for descriptive purposes only and does not imply endorsement by the U.S. Government.

\* The use of trade names does not signify endorsement by the U.S. Geological Survey.

## Data availability

All data are made available in the Supplementary Information associated with the publication. We include detailed materials and methods (S1 Appendix), complete processed Dataset (S2 Dataset), a compilation of microphotographs of the FI and crystals (S3 FI Image Compilation) and a record of emails and tracking receipts related to the samples, data sharing and manuscript submission (S4 Email and tracking record). All raw data and Jupyter notebooks are also stored on Github ([https://github.com/cljdevitre/2023\\_Kilauea-rapid-response-simulation](https://github.com/cljdevitre/2023_Kilauea-rapid-response-simulation)). The Github repository will be archived on Zenodo upon acceptance.

## References

- Anderson, K. R., Johanson, I. A., Patrick, M. R., Gu, M., Segall, P., Poland, M. P., Montgomery-Brown, E. K. & Miklius, A. (2019). Magma reservoir failure and the onset of caldera collapse at Kīlauea Volcano in 2018. *Science*. American Association for the Advancement of Science **366**, eaaz1822.
- Anderson, K. R. & Poland, M. P. (2016). Bayesian estimation of magma supply, storage, and eruption rates using a multiphysical volcano model: Kīlauea Volcano, 2000–2012. *Earth and Planetary Science Letters* **447**, 161–171.
- Baker, S. & Amelung, F. (2012). Top-down inflation and deflation at the summit of Kīlauea Volcano, Hawai‘i observed with InSAR. *Journal of Geophysical Research: Solid Earth* **117**.
- Dayton, K. *et al.* (2023). Deep magma storage during the 2021 La Palma eruption. *Science Advances*. American Association for the Advancement of Science **9**, eade7641.
- DeVitre, C. L., Allison, C. M. & Gazel, E. (2021). A high-precision CO<sub>2</sub> densimeter for Raman spectroscopy using a Fluid Density Calibration Apparatus. *Chemical Geology* **584**, 120522.

\* The use of trade names does not signify endorsement by the U.S. Geological Survey.

- DeVitre, C. L. & Wieser, P. (2023). Reliability of Raman analyses of CO<sub>2</sub>-rich fluid inclusions as a rapid barometer at Kīlauea. *EarthArXiv*.
- Ganseccki, C., Lee, R. L., Shea, T., Lundblad, S. P., Hon, K. & Parcheta, C. (2019). The tangled tale of Kīlauea's 2018 eruption as told by geochemical monitoring. *Science*. American Association for the Advancement of Science **366**, eaaz0147.
- Helz, R. T., Clague, D. A., Sisson, T. W. & Thornber, C. R. (2014). *Petrologic insights into basaltic volcanism at historically active Hawaiian volcanoes. Characteristics of Hawaiian volcanoes*. US Geological Survey, Professional Papers, 237–294.
- Lerner, A. H. *et al.* (2021). The petrologic and degassing behavior of sulfur and other magmatic volatiles from the 2018 eruption of Kīlauea, Hawai'i: melt concentrations, magma storage depths, and magma recycling. *Bulletin of Volcanology*. Springer **83**, 1–32.
- Mourey, A. J., Shea, T., Costa, F., Shiro, B. & Longman, R. J. (2023). Years of magma intrusion primed Kīlauea Volcano (Hawai'i) for the 2018 eruption: evidence from olivine diffusion chronometry and monitoring data. *Bulletin of Volcanology* **85**, 18.
- Pankhurst, M. J. *et al.* (2022). Rapid response petrology for the opening eruptive phase of the 2021 Cumbre Vieja eruption, La Palma, Canary Islands. *Volcanica* **5**, 1–10.
- Pietruszka, A. J., Heaton, D. E., Marske, J. P. & Garcia, M. O. (2015). Two magma bodies beneath the summit of Kīlauea Volcano unveiled by isotopically distinct melt deliveries from the mantle. *Earth and Planetary Science Letters* **413**, 90–100.
- Pietruszka, A. J., Marske, J. P., Heaton, D. E., Garcia, M. O. & Rhodes, J. M. (2018). An Isotopic Perspective into the Magmatic Evolution and Architecture of the Rift Zones of Kīlauea Volcano. *Journal of Petrology* **59**, 2311–2352.
- Re, G., Corsaro, R. A., D'Orlando, C. & Pompilio, M. (2021). Petrological monitoring of active volcanoes: A review of existing procedures to achieve best practices and operative protocols during eruptions. *Journal of Volcanology and Geothermal Research* **419**, 107365.
- Ryan, M. P. (1987). The elasticity and contractancy of Hawaiian olivine tholeiite, and its role in the stability and structural evolution of sub-caldera magma reservoirs and rift systems. In *Volcanism in Hawaii*. *US Geol. Surv. Prof. Pap.* **1350**, 1395–1447.
- Span, R. & Wagner, W. (1996). A new equation of state for carbon dioxide covering the fluid region from the triple-point temperature to 1100 K at pressures up to 800 MPa. *Journal of physical and chemical reference data*. American Institute of Physics for the National Institute of Standards and ... **25**, 1509–1596.
- Welsch, B., Faure, F., Famin, V., Baronnet, A. & Bachèlery, P. (2013). Dendritic Crystallization: A Single Process for all the Textures of Olivine in Basalts? *Journal of Petrology* **54**, 539–574.
- Wieser, P. E. *et al.* (2021). Reconstructing Magma Storage Depths for the 2018 Kīlauean Eruption From Melt Inclusion CO<sub>2</sub> Contents: The Importance of Vapor Bubbles. *Geochemistry, Geophysics, Geosystems* **22**, e2020GC009364.

\* The use of trade names does not signify endorsement by the U.S. Geological Survey.

- 252 Wieser, P. E., Edmonds, M., MacLennan, J., Jenner, F. E. & Kunz, B. E. (2019). Crystal  
253 scavenging from mush piles recorded by melt inclusions. *Nature Communications*.  
254 Nature Publishing Group **10**, 5797.
- 255 Wieser, P. E., Kent, A. J. R. & Till, C. B. (2023a). Barometers Behaving Badly II: a Critical  
256 Evaluation of Cpx-Only and Cpx-Liq Thermobarometry in Variably-Hydrous Arc  
257 Magmas. *Journal of Petrology* **64**, egad050.
- 258 Wieser, P. E., Kent, A., Till, C. & Abers, G. (2023b). Geophysical and Geochemical Constraints  
259 on Magma Storage Depths along the Cascade Arc: Knowns and Unknowns. EarthArXiv.
- 260
- 261

\* The use of trade names does not signify endorsement by the U.S. Geological Survey.

## Figure captions

### **Figure 1. Workflow of the study, all times on this figure are Pacific Standard Time (PST).**

Stick people show the contribution of individual team members, to indicate the total time associated with each step. We note that AB was trained in these procedures during the simulation and all reports were sent to HVO prior to 5:30 pm Hawaii Standard Time (HST), thus allowing for decision making for the following day.

**Figure 2. Evolution of results over 4 days.** a) Schematic model of Kīlauea's plumbing system, indicating reservoir depths determined by geophysics and prior petrological work (HMM- Halema'uma'u; SC – South Caldera). b) By the end of Day 1, FI revealed that the crystals were supplied from depths consistent with the Halema'uma'u reservoir. Kolmogorov-Smirnov tests show that September 2023 FI are recording depths significantly shallower than those recorded by FI (critical  $D = 0.22$ ,  $\text{stat} = 0.24$ ,  $\text{pval} = 0.016$ ) and MI (critical  $D = 0.22$ ,  $\text{stat} = 0.41$ ,  $\text{pval} = 3.51\text{e-}06$ ) from the 2018 lower East Rift Zone eruption, which required a contribution from the South Caldera reservoir. <sup>1</sup> Melt inclusion data for the 2018 LERZ eruption is from Wieser *et al.*, (2021); <sup>2</sup> Fluid inclusion data for the 2018 LERZ eruption is from DeVitre and Wieser, (2023) c) By the end of Day 2, depths from 46 FI were sent to HVO, confirming a dominant role of the Halema'uma'u reservoir. On Day 2 we applied a conservative degassing filter ( $\text{SO}_2$  mol% < 2.5). d) By the end of Day 4, after taking a mean of repeated analyses of single FI, applying more stringent data filters, using FI-specific temperatures, and a more appropriate crustal model (density of  $\sim 2300 \text{ kg/m}^3$  with a normal error distribution of  $100 \text{ kg/m}^3$ ), entrapment depths with uncertainties were linked to crystal chemistry. Error bars correspond to uncertainties propagated using Monte Carlo simulations (see Supplementary Information S1 Appendix)

\* The use of trade names does not signify endorsement by the U.S. Geological Survey.

Olivine Fo equilibrium field is calculated based on Glass EPMA data collected on September 11, 2023 (see Supplementary Information S1 Appendix). We note here that initial data for Days 1 and 2 did not filter out repeated analyses (1 repeated FI in Day 1 and 6 in Day 2), pressures were calculated using an estimated entrapment temperature of 1150°C (Wieser *et al.*, 2021; DeVitre and Wieser, 2023), and depth was calculated using the model of (Ryan, 1987) described in (Lerner *et al.*, 2021) for crustal density.

\* The use of trade names does not signify endorsement by the U.S. Geological Survey.

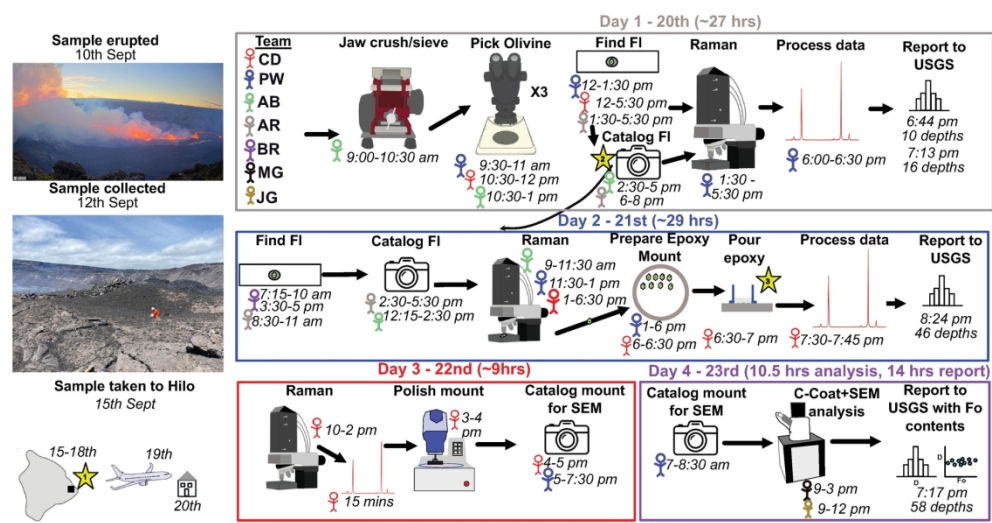


Figure 1. Workflow of the study, all times on this figure are Pacific Standard Time (PST). Stick people show the contribution of individual team members, to indicate the total time associated with each step. We note that AB was trained in these procedures during the simulation and all reports were sent to HVO prior to 5:30 pm Hawaii Standard Time (HST), thus allowing for decision making for the following day.

168x87mm (300 x 300 DPI)



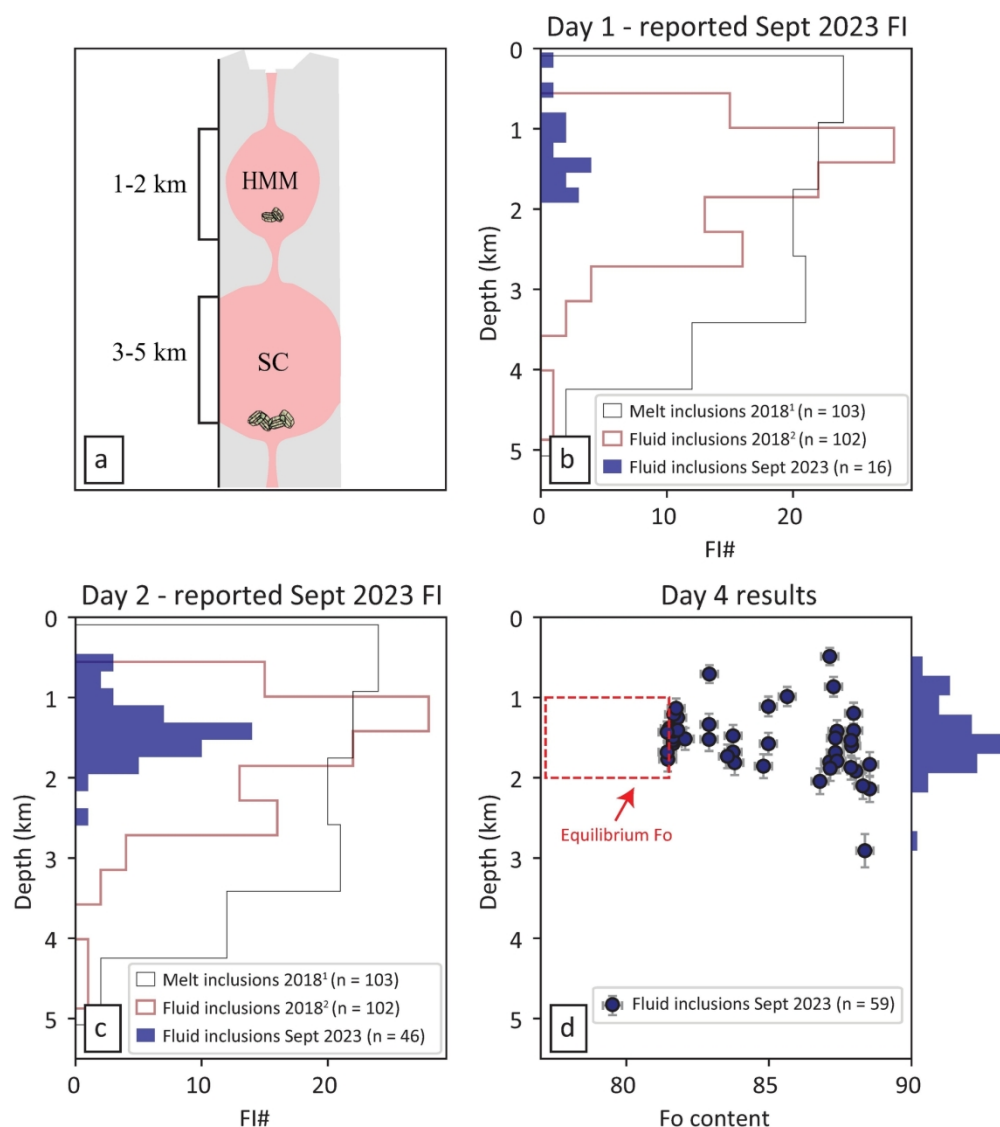


Figure 2. Evolution of results over 4 days. a) Schematic model of Kilauea's plumbing system, indicating reservoir depths determined by geophysics and prior petrological work (HMM- Halema'uma'u; SC – South Caldera). b) By the end of Day 1, FI revealed that the crystals were supplied from depths consistent with the Halema'uma'u reservoir. Kolmogorov-Smirnov tests show that September 2023 FI are recording depths significantly shallower than those recorded by FI (critical  $D = 0.22$ ,  $stat = 0.24$ ,  $pval = 0.016$ ) and MI (critical  $D = 0.22$ ,  $stat = 0.41$ ,  $pval = 3.51e-06$ ) from the 2018 lower East Rift Zone eruption, which required a contribution from the South Caldera reservoir. 1 Melt inclusion data for the 2018 LERZ eruption is from Wieser et al., (2021); 2 Fluid inclusion data for the 2018 LERZ eruption is from DeVitre and Wieser, (2023) c) By the end of Day 2, depths from 46 FI were sent to HVO, confirming a dominant role of the Halema'uma'u reservoir. On Day 2 we applied a conservative degassing filter ( $SO_2$  mol% < 2.5). d) By the end of Day 4, after taking a mean of repeated analyses of single FI, applying more stringent data filters, using FI-specific temperatures, and a more appropriate crustal model (density of  $\sim 2300$  kg/m<sup>3</sup> with a normal error distribution of 100 kg/m<sup>3</sup>), entrapment depths with uncertainties were linked to crystal chemistry. Error bars correspond to uncertainties propagated using Monte Carlo simulations (see Supplementary Information S1 Appendix) Olivine Fo equilibrium field is calculated based on Glass EPMA data

collected on September 11, 2023 (see Supplementary Information S1 Appendix). We note here that initial data for Days 1 and 2 did not filter out repeated analyses (1 repeated FI in Day 1 and 6 in Day 2), pressures were calculated using an estimated entrapment temperature of 1150°C (Wieser et al., 2021; DeVitre and Wieser, 2023), and depth was calculated using the model of (Ryan, 1987) described in (Lerner et al., 2021) for crustal density.

166x186mm (300 x 300 DPI)